

Journal of Materials Chemistry B

Accepted Manuscript

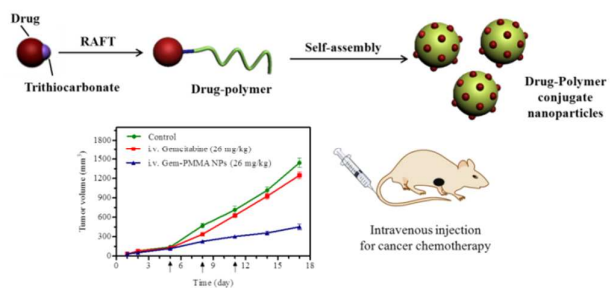


This is an *Accepted Manuscript*, which has been through the Royal Society of Chemistry peer review process and has been accepted for publication.

Accepted Manuscripts are published online shortly after acceptance, before technical editing, formatting and proof reading. Using this free service, authors can make their results available to the community, in citable form, before we publish the edited article. We will replace this *Accepted Manuscript* with the edited and formatted *Advance Article* as soon as it is available.

You can find more information about *Accepted Manuscripts* in the [Information for Authors](#).

Please note that technical editing may introduce minor changes to the text and/or graphics, which may alter content. The journal's standard [Terms & Conditions](#) and the [Ethical guidelines](#) still apply. In no event shall the Royal Society of Chemistry be held responsible for any errors or omissions in this *Accepted Manuscript* or any consequences arising from the use of any information it contains.



Novel prodrug nanoparticles with tailorable high drug payloads and in vivo anticancer activity assembled from well-defined gemcitabine-polymer conjugate amphiphiles prepared by RAFT polymerization are presented.

Tailor-made gemcitabine prodrug nanoparticles from well-defined drug-polymer amphiphiles prepared by controlled living radical polymerization for cancer chemotherapy

Weiwei Wang¹, Chen Li¹, Ju Zhang¹, Anjie Dong², Deling Kong^{1*}

¹Tianjin Key Laboratory of Biomaterial Research, Institute of Biomedical Engineering, Chinese Academy of Medical Science and Peking Union Medical College, Tianjin, 300192, China

²School of Chemical Engineering and Technology, Tianjin University, Tianjin, 300072, China

Abstract

The therapeutic efficacy of gemcitabine is severely compromised by its rapid plasma degradation and low tumor-targeting efficiency. Furthermore, the hydrophilic property of gemcitabine also makes efficient encapsulation and in vivo release of the compound difficult in a nanoscale drug delivery system. Herein, gemcitabine-poly(methyl methacrylate) (Gem-PMMA) conjugated amphiphiles were prepared from the gemcitabine-bearing trithiocarbonate initiator via reversible addition-fragmentation chain transfer (RAFT) polymerization. The prodrug conjugate with high drug payload can self-assemble in water into nanoparticles with an average diameter of 130 nm. In addition, gemcitabine molecules within the Gem-PMMA nanoparticles mainly existed in amorphous, implicating better gemcitabine release. Indeed, the releasing kinetics of gemcitabine was pH-dependent and a controlled release of gemcitabine from the nanoparticles was observed with 71.6% of cumulative drug release in 72h in the

Corresponding to: Prof. Deling Kong, Email: kongdeling@nankai.edu.cn

presence of protease Cathepsin B. Cytotoxicity of the gemcitabine prodrug nanoparticles was evident as demonstrated by in vitro viability assay using human pulmonary carcinoma, A549, and breast cancer cells, MCF-7. In vivo assessment of the gemcitabine-loaded nanoparticles using BALB/c nude mice with A549 cell-derived xenograft tumors indicated these intravenously administered nanoparticles efficiently inhibited tumor growth as well as alleviated the drug-associated side effects at a dose of 26 mg/kg. In summary a prodrug nanoparticle, Gem-PMMA, with excellent delivery efficiency and tumor growth inhibition efficacy, was designed and produced. Our results demonstrated the potential of the gemcitabine prodrug nanoparticles as a promising therapeutic formulation for chemotherapy.

Keywords: gemcitabine, RAFT polymerization, prodrug conjugate, nanoparticle, cancer chemotherapy

1. Introduction

Malignancy is currently the second major cause of global deaths. Increasing research effort has focused on designing drug-loaded polymeric nanoparticles, which may provide effective means in clinical targeting of cancers as well as other diseases.¹⁻⁷ These nanoconstructs could be commonly obtained by encapsulation of a certain drug compound during aqueous self-assembly of amphiphilic copolymers, which improves aqueous solubility of hydrophobic drugs. This approach also stabilizes the chemical activity of medical compounds, enhances permeability and retention (EPR) effect, resulting in increased systemic circulation period and drug

targeting respectively.⁸ However, several limitations of this drug delivery approach have been reported that may hamper the clinical efficacy of chemotherapy. Premature burst release is one of the limiting factors that may cause adverse side effects and danger to patients by rapid release of encapsulated chemotherapeutic agent before reaching its designated tumor target. Another detrimental factor is a high tendency of poorly soluble drugs to crystallize within the hydrophobic core of nanoparticles during encapsulation, which can inhibit drug release in the targeted tissues. Moreover, the efficiency of maximum drug encapsulation is only a few percent due to self-interaction of the medical agents as well as interactions between drugs and the hydrophobic core of the nanoparticles. The resulted low delivery efficiency in turn requires a large amount of nanocarriers, which is a common health concern. Lastly, encapsulation of aqueous soluble drugs into nano-sized delivery systems is a highly difficult and complex process. Even when encapsulation has been successful, a sustainable drug release is usually hard to achieve. Given the limitations of the current nanocarriers, other means to facilitate targeted drug delivery has been investigated. The engineering of prodrug has been considered as an alternative.⁹⁻¹⁸ Promising results from clinical trials using macromolecule-drug conjugates (e.g., albumin-bound paclitaxel^{19, 20}) reported better anticancer efficacy, further supporting the suggestion of using other synthetic polymers as delivery vehicles for drug targeting.

Prodrugs are biologically reversible derivatives of intended drug compounds. After administration, they could undergo enzymatic or chemical transformation to release active parent drugs, which could then exert the desired pharmacological effects in

vivo. In terms of polymeric prodrug synthesis, the commonly used approach is to chemically attach hydrophobic drugs to a prefabricated hydrophilic polymer such as poly(ethylene glycol),^{21, 22} poly(L-glutamic acid),¹³ poly(N-2-hydroxypropyl-methacrylamide),²³ or dextran²⁴ to produce fully water-soluble conjugates or small-sized aggregates in an aqueous environment. This strategy has the potential to overcome limitations such as low drug payload, rapid pre-systemic metabolism and toxicity that are commonly observed of the drug delivery system using encapsulative nanocarriers.²⁵⁻²⁹ Similar approach has been reported by conjugating pharmaceutical agents to amphiphilic copolymers, which also showed improvements in drug delivery.^{2, 14, 30-32} However, some major issues still remain to be considered, including how to maximize drug loading and precisely regulate drug payload. Currently, for water-soluble drugs, some efforts have been made to their hydrophobic modification to facilitate the encapsulation into another nanoparticle or liposome carrier,^{9, 33} however, this method inhibits effective drug release, its subsequent diffusion and permeation into targeted tumors.

Herein, a new category of anti-cancer prodrug nanocarriers have been generated with tailor-made high drug payload and delivery efficiency. These prodrug nanoparticles were assembled from amphiphilic drug-polymer conjugates that are obtained via reversible addition-fragmentation chain transfer (RAFT) polymerization, a controlled living radical polymerization technique. In this study, we report a new approach by conjugating the intended drug molecule to a gemcitabine (Gem)-bearing trithiocarbonate initiator, from which a polymer chain composed of poly (methyl

methacrylate) (PMMA) oligomer could be produced in a highly regulated manner. In this way, an amphiphilic drug-polymer conjugate could be generated with the hydrophilic drug molecule at the end of a hydrophobic polymer long chain (Scheme 1). The amphiphilic nature of the drug-polymer conjugates would subsequently propel self-assembly of these prodrug amphiphiles to form nanoscale aggregates in aqueous environment, by which drug loading and delivery could be achieved. The chemical structure of the drug-polymer conjugate was characterized by ^1H NMR and gel permeation chromatography (GPC). Dynamic light scattering (DLS) and transmission electron microscopy (TEM) were employed to assess the physical characteristics and morphology of the drug-polymer nanoparticles in water. The thermodynamic state of the drug molecules was examined using differential scanning calorimetry (DSC) and X-ray diffraction (XRD). Drug releasing profile from the prodrug conjugate and its cytotoxicity were determined by *in vitro* assays using human pulmonary carcinoma A549 and breast cancer cells MCF-7. The efficiency and efficacy of drug delivery of the prodrug was also investigated by *in vivo* analysis following intravenous injection of the prodrug nanoparticles in mice that have developed advanced breast cancer.



Scheme 1. The strategy to achieve well-defined polymer–drug conjugate nanoparticles by reversible addition–fragmentation chain transfer (RAFT) polymerization.

2. Materials and Experiments

2.1 Materials

Gemcitabine hydrochloride (Gem·HCl), hexylamine, 1-(3-dimethylaminopropyl)-3-ethylcarbodiimide hydrochloride (EDC·HCl) and N-hydroxysuccinimide (NHS) were used as received from Sigma-Aldrich. □Methyl methacrylate (MMA) from Sigma-Aldrich was distilled under reduced pressure to eliminate the inhibitor prior to use. The RAFT agent precursor *S*-1-dodecyl-*S'*-(α,α' -dimethyl- α'' -acetic acid) trithiocarbonate was synthesized according to the previous method.³⁴ Tetrahydrofuran (THF) and dimethyl sulfoxide (DMSO) were obtained from Jiangtian chemical company and distilled over sodium/benzophenone before use. Dimethyl formamide (DMF) was dried over magnesium sulfate and distilled under reduced pressure just before use.

2.2 Synthesis of Gem-terminated trithiocarbonate

The RAFT agent, gem-terminated trithiocarbonate was prepared through the amidation of amino on gemcitabine molecule and carboxyl on *S*-1-dodecyl-*S'*-(α,α' -dimethyl- α'' -acetic acid) trithiocarbonate. The synthesis route is shown in scheme 1. Generally, Gem·HCl (300 mg, 1 mmol) was firstly dissolved in dry DMF with triethylamine (139 μ L, 1 mmol). *S*-1-dodecyl-*S'*-(α,α' -dimethyl- α'' -acetic acid) trithiocarbonate (364 mg, 1 mmol) was also dissolved in dry DMF and activated with EDC/NHS for 2 h. Then the gemcitabine solution was added into the above mixture and the reaction was performed at room temperature for 24 h. The

crude products were diluted with ethyl acetate, washed with 10% hydrochloric acid, saturated NaHCO_3 and brine, and dried over MgSO_4 . The solvent was removed under vacuum and the product was further separated by chromatography on silica using 20% petroleum ether in ethyl acetate as eluent. Yield: 347 mg, yellow solid (0.569 mmol, 52.3%). ^1H NMR ($\text{DMSO}-d_6$, 500 MHz): δ 10.27 (s, 1H, CONH), 8.03 (d, 1H, H-a'), 7.47 (d, 1H, H-b'), 6.21 (d, 1H, H-c'), 5.83 (s, 1H, H-d'), 5.30 (t, 1H, H-e'), 4.30 (m, 4H, H-f'-h'), 3.28 (m, 2H, $-\text{SCS}_2\text{CH}_2-$), 1.60 (m, 4H, $-\text{NHCOC}(\text{CH}_3)_2-$), 1.22 (m, 20H, $-\text{SCS}_2\text{CH}_2(\text{CH}_2)_{10}\text{CH}_3$), 0.84 (s, 3H, $-\text{SCS}_2\text{CH}_2(\text{CH}_2)_{10}\text{CH}_3$).

2.2 Synthesis of Gem-PMMA conjugates

RAFT polymerization was employed to prepare Gem-PMMA prodrug conjugates. A typical procedure was as follows: MMA (600 mg, 6 mmol), Gem-RAFT (305 mg, 0.5 mmol) and 2,2'-azodiisobutyronitrile (8.2 mg, 0.05 mmol) were dissolved in 2 mL of dimethyl sulfoxide. The mixture was degassed by three cycles of freeze-pump-thaw and sealed with argon. After stirred at 60 °C for 12 h, the crude product was precipitated in excess diethyl ether to give the precursor Gem-PMMA as light yellow powders. Then Gem-PMMA (173 mg, 0.1 mmol) was redissolved in dimethyl sulfoxide (2 mL), and hexylamine (51 mg, 0.5 mmol) was added to the solution. The reaction mixture was stirred for 1 h at room temperature under a nitrogen atmosphere. After precipitated in diethyl ether, filtered and dried in vacuum, the final Gem-PMMA was harvested as colorless powders. The polymerization degree of MMA and the aminolysis of the thiocarbonylthio groups were confirmed by ^1H

NMR (Varian INOVA 500MHZ, solvent: DMSO- d_6) and gel permeation chromatography (GPC, Viscotek GPCmax, Malvern).

2.3 Characterization of gemcitabine in Gem-PMMA

The physical state of gemcitabine in Gem-PMMA conjugates was investigated using DSC (NETSCZ 204, Germany) and XRD (Bruker D8-S4, Germany). Gem-PMMA powders were subjected to DSC and XRD with native gemcitabine as control. For DSC measurement the heating rate was 10 °C/min in the temperature range of 30-200°C, whereas for X-ray diffraction the diffraction angle 2θ was recorded from 6° to 60° with a scanning speed of 10°/min and copper was used as the source of x-ray radiation at 40 Kv with 40 mA.

2.4 Self-assembly and characterization of Gem-PMMA conjugates in water

Due to the amphiphilic nature of Gem-PMMA, the self-assembly of nanoparticles were prepared using the nanoprecipitation technology. Typically, twenty milligrams of Gem-PMMA were dissolved in 4 mL of dimethyl sulfoxide and the resulted solution was slowly dropwised into 20 mL of ultrapure water. Dimethyl sulfoxide was removed by dialysis. The final Gem-PMMA concentration was adjusted to 1 mg/mL.

The hydrodynamic size of Gem-PMMA nanoparticles in water was studied by a dynamic light scattering (DLS) instrument (Brookhaven BI-200SM, USA) at $\lambda = 532$ nm under room temperature. Measurements of scattered light were fixed at an angle of 90° to the incident beam. The results of DLS were analyzed by the regularized

CONTIN method. The zeta potential of Gem-PMMA particles in water was determined using a Malvern Zetasizer Nano ZS (Malvern Instruments Ltd., MA). The morphology and core size of Gem-PMMA nanoparticles were determined by a JEM-2100F transmission electron microscope at an accelerating voltage of 200 kV.

2.5 *In vitro* drug release

In vitro release of gemcitabine from polymer-drug conjugate nanoparticles was investigated with or without the protease Cathepsin B (5 U/mL). Gem-PMMA conjugates were formulated in acetate buffer (20 mL, pH 5.0) containing 400 μ L of enzyme or PBS buffer (20 mL, pH 6.8 or 7.4). Samples in dialysis tubes were prepared in triplicate and shaken at 100 rpm at 37 °C. At regular time intervals, samples (3 mL) were withdrawn and the content of free or conjugated gemcitabine was analyzed by UV spectrum. Then the cumulative release of gemcitabine was calculated.

2.6 Cell culture

Human lung carcinoma cell line (A549) was obtained from Sigma-Aldrich and human breast adenocarcinoma cell line (MCF-7) was kindly provided by Professor Anli Jiang from Institute of Biochemistry and Molecular Biology, Medical School of Shandong University. A549 cells were maintained in Hyclone Ham's/F12 medium. MCF-7 cells were cultured in Hyclone DMEM/High Glucose medium. All media were supplemented with 10% heat-inactivated fetal bovine serum (FBS), penicillin

(100 U/mL) and streptomycin (100 $\mu\text{g/mL}$). All cell lines were maintained at 37 °C and 5% CO₂ in humidified atmosphere.

2.7 In vitro and in vivo anti-tumor activity of gemcitabine

The in vitro cytotoxicity of free gemcitabine or Gem-PMMA conjugate nanoparticles was evaluated on the above two cells lines by cell counting kit-8 (CCK-8) viability test. Briefly, cells were seeded in 100 μL of culture medium (5×10^3 cells/well) in 96-well microtiter plates and pre-incubated for 24 h. The cells were then exposed to a series of gemcitabine or Gem-PMMA solutions of different concentrations for 48 h. After incubation, 10 μL of CCK-8 (Dojindo, Japan) solution in phosphate-buffered saline was added to each well. After incubation for 60 min, the absorbance of the solubilized dye was measured spectrophotometrically with a microplate reader (Thermo Scientific Varioskan Flash) at 450 nm. The percentage of viable cells in each well was calculated as the absorbance ratio between treated and untreated control cells. All experiments were set up in quintuplicate to determine mean values and standard deviations (SDs).

The in vivo anti-tumor activity was conducted using xenograft tumor models. All animal experiments were performed in accordance with the protocol approved by Tianjin Institute of Medical and Pharmaceutical Science. Xenograft tumors were subcutaneously implanted in 6-7 weeks old male BALB/c nude mice (Vital River Laboratory Animal Technology Co. Ltd, China) by the injection of 200 μL of A549 cells (2×10^6) suspension in the upper portion of the right flank. The treatment was

initiated when the tumor reached approximate 100~150 mm³. The mice were randomly assigned to one of the three treatment groups. Group 1 (n=10), mice were untreated as control group; group 2 (n=10), mice received intravenous injection of gemcitabine (26 mg/kg); group 3 (n=10), mice received intravenous administration of Gem-PMMA (26 mg/kg). The tumor volumes were measured using a caliper and calculated according to the formula, tumor volume = $a^2 \times b / 2$, where a is the shorter diameter and b is the longer one. Body weight of the animals was also recorded every two days. The statistical difference was analyzed by one-way ANOVA method and the results were expressed as mean \pm SD. $p < 0.05$ were considered as significant.

3. Results

3.1. Synthesis and characterization of gemcitabine-poly (methyl methacrylate) (Gem-PMMA) conjugates

Gemcitabine is a nucleoside analogue, which acts against a wide range of solid tumors, including pancreatic, non-small lung, breast, and ovarian.^{10, 35, 36} Clinical trials using gemcitabine for melanoma therapy have also been reported.³⁷ Despite its effective anti-cancer activity, gemcitabine suffers from various drawbacks, such as rapid deamination to inactive 2',2'-difluorodeoxyuridine by cytidine deaminase after intravenous injection, resulting in a short in vivo half-life (8–17 min).⁹ Furthermore, a lower level of transportation of gemcitabine into cells resulted from blocked uptake due to decreased expression of different transporters, such as hENT1, also restricts its anti-cancer activity.³⁵ Therefore, a strategy that both provides protection of the amino

on 4-(N)-site and enhanced transport by chemical modification of the gemcitabine molecule could potentially lead to novel therapeutic formulations. Inspired by this, the preparation of gemcitabine prodrug nanoparticles was proposed and the RAFT technique, which offers incomparable flexibility in the construction of advanced macromolecular architectures, was performed to prepare the gemcitabine-poly (methyl methacrylate) (Gem-PMMA) conjugate macromolecules. The synthesis route is depicted in Fig. 1. The gemcitabine end functionalized poly (methyl methacrylate) was synthesized from the polymerization of methyl methacrylate (MMA) under traditional radical initiation in the presence of the Gem-based trithiocarbonate RAFT agent. As an initial step, the trithiocarbonate RAFT moiety *S*-1-Dodecyl-*S'*-(α,α' -dimethyl- α'' -acetic acid) was synthesized. Then gemcitabine was chemically conjugated to it through the amidation of the 4-(N)-site amino of gemcitabine and the carboxyl of trithiocarbonate moiety using the EDC/NHS coupling chemistry. As amino is more prone to react with carboxyl compared to hydroxyl, the selectivity and yield of the conjugation procedure were acceptable.

The RAFT polymerization of MMA was carried out in anhydrous DMSO at 60 °C under azodiisobutyronitrile radical initiation and Gem-PMMA with low dispersity and controlled hydrophobic segment length was obtained. By varying the feeding amount of MMA monomers, two representative Gem-PMMA with tailor-made and high drug payload were constructed as shown in Table 1. The chemical structure of Gem-PMMA was firstly confirmed by ^1H NMR (Fig. 2). The characteristic proton peaks in the chemical shift range of 4.0-9.0 ppm attributed to Gem, protons peak at

$\delta=3.55$ ppm ascribed to the methyl of PMMA and that at $\delta=1.21$ ppm assigned to methylenes of the initiator all appear in the ^1H NMR spectra, which confirm the successful polymerization of MMA. In order to eliminate the potential biological toxicity of trithiocarbonates and obtain a functional living thiol group, a subsequent aminolysis was performed to break the thiocarbonylthio group. The disappearance of proton peaks at δ 0.83, 1.21 and 3.20 ppm assigned to methylene and methyl of dodecyl demonstrated the complete fragmentation of the thiocarbonylthio moiety. The molecular weight of hydrophobic PMMA in Gem-PMMA calculated from ^1H NMR was 500 and 1120, respectively. Thus, the corresponding gemcitabine weight fractions in Gem-PMMA conjugates were 43.7 and 21.5wt%, respectively. Furthermore, the molecular weight distribution detected by GPC was approximate 1.2. An advantage of the synthetic strategy of growing MMA from the Gem-based RAFT agent is that the weight fraction of gemcitabine in the resulting conjugate can be fine-tuned by adjusting the hydrophobic polymer chain length through altering the initial stoichiometry of the monomers. Significantly, the drug payload could be easily increased to over 20 wt% by reducing the polymer chain length, which is certainly owe to the controlled living radical polymerization technique implemented here.

The chemical conjugation of gemcitabine was further determined by UV-Vis spectroscopy. As depicted in Fig. S1 (Supplementary data), the maximum absorption peak of native gemcitabine appeared at the wavelength of 268 nm, however, that of gemcitabine in Gem-PMMA conjugates was around 305 nm. This red shift of wavelength indicated that gemcitabine was chemically linked to PMMA by amide

bond, which has a stronger electronegativity compared to amino.³⁸⁻⁴⁰ The prominent difference in ultraviolet absorption of free or conjugated gemcitabine was then utilized to characterize the hydrolysis of Gem-PMMA under the catalysis of cathepsin.

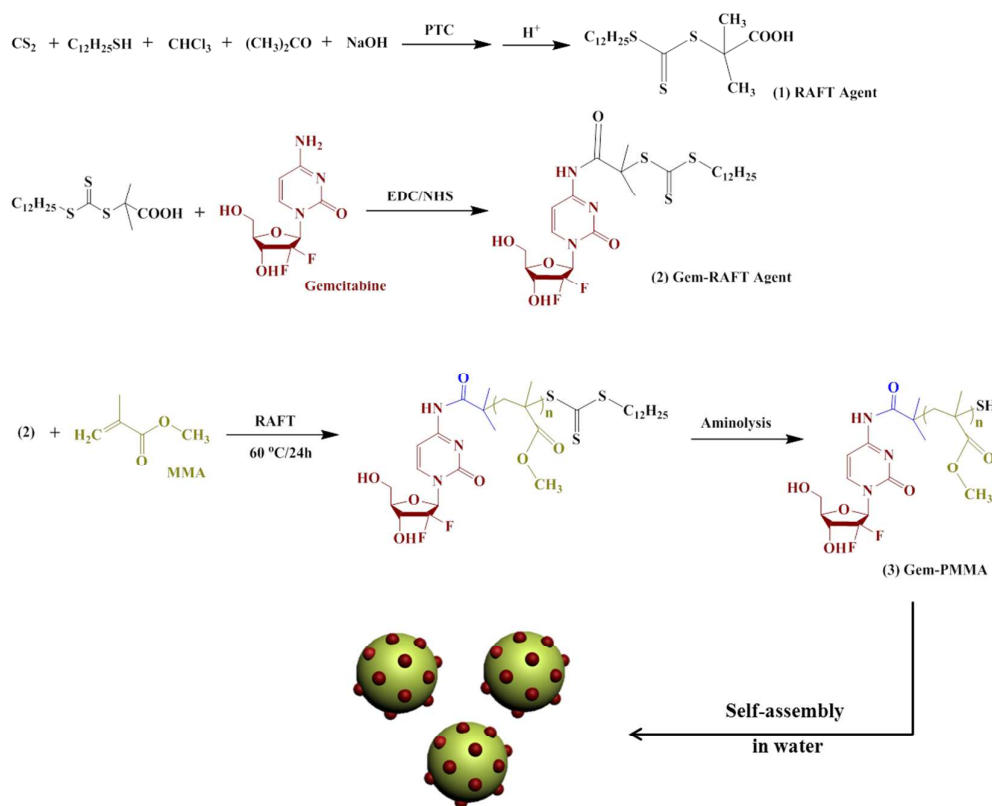


Figure 1. The design of Gem-PMMA conjugate nanoparticles.

Table 1. Characterization of gemcitabine–poly (methyl methacrylate) (Gem-PMMA) conjugates and nanoparticles.

Gem-PMMA	M_n ^[a] (g/mol)	PDI ^[b]	Size ^[c] (nm)	PDI ^[c]	ζ ^[d] (mV)	%Gem ^[e] (wt %)
Gem-PMMA5	865	1.23	123 ± 3	0.13	-65.3	43.7
Gem-PMMA11.2	1485	1.21	136 ± 4	0.14	-64.9	21.5

[a] Determined by ¹H-NMR. [b] Detected by GPC. [c] Determined by DLS. [d] Zeta potential determined by Zetasizer (Malven). [e] %Gem = $M_n(\text{Gem})/M_n(\text{PMMA})$.

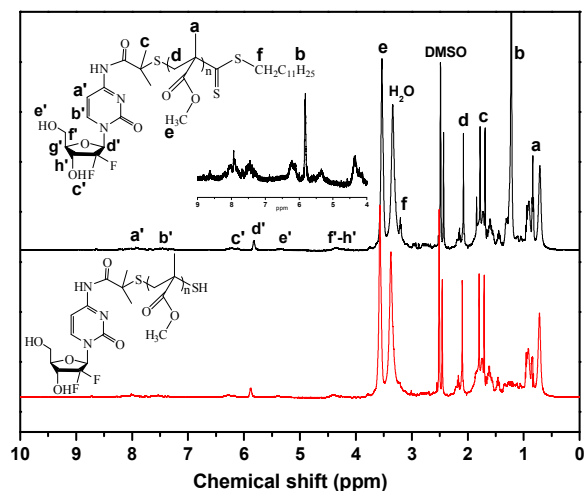


Figure 2. The ^1H NMR spectra of Gem-PMMA conjugates.

3.2 Characterization of gemcitabine in Gem-PMMA

The physical state of drug in nanoparticle or other formulations can influence the drug loading capacity, the homogeneity of drug in formulation, the stability of formulation as well as the therapeutic effect.^{41, 42} Generally, drugs encapsulated in the hydrophobic core of nanoparticles with a high drug payload tended to crystallize, which could inhibit the effective and complete release of drug.³⁴ Conversely, increasing the amorphous fraction of drug can improve the sustained release of drug. Therefore, the state of gemcitabine in Gem-PMMA conjugates was analyzed by DSC and XRD. As can be seen from Fig. 3A, the melting endotherm of pure gemcitabine appeared at 168 °C, nevertheless, no obvious melting peak of gemcitabine was detected for Gem-PMMA conjugates even with a drug payload as high as 43.7 %wt. It can thus be concluded that gemcitabine in Gem-PMMA was in amorphous. The information obtained from XRD (Fig. 3B) complied with the results obtained from

DSC analysis. The disappearance of characteristic crystalline peak of gemcitabine suggested that gemcitabine in Gem-PMMA was in amorphous state, which would avoid the above-mentioned undesirable outcomes resulted from drug crystallization.

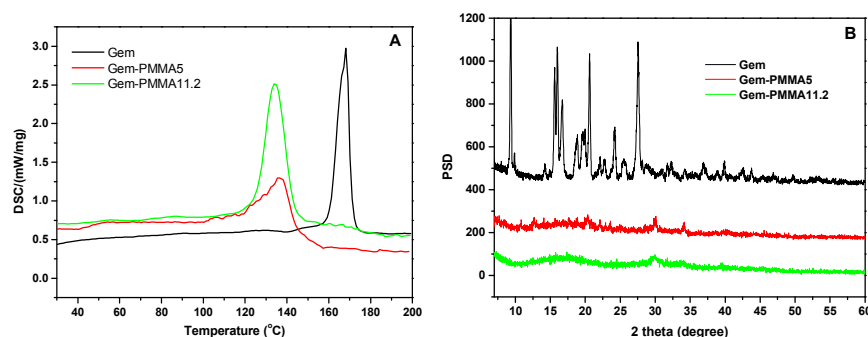


Figure 3. The DSC and XRD curves of gemcitabine and Gem-PMMA conjugates.

3.3 Formation and characterization of Gem-PMMA nanoparticles in water

Due to the amphiphilic nature of the macromolecular conjugates, nanoprecipitation technique was performed without any additional stabilizer to prepare Gem-PMMA nanoparticles by the self-assembly of Gem-PMMA conjugates in aqueous solution. The hydrodynamic size and morphology of obtained nanoparticles were characterized by DLS and TEM (Fig. 4). The average diameters for Gem-PMMA5 and Gem-PMMA11.2 nanoparticles were 123 nm and 136 nm, respectively, which are suitable for intravenous administration. The zeta potential for conjugate polymers was around -65 mV. No clear dependence of the nanoparticle size and the surface zeta potential on the polymer chain length was observed. The distribution indexes of both nanoparticles were all below 0.15 as determined by DLS, indicating a monodispersity system. Prodrug nanoparticles were further characterized by TEM and the images showed Gem-PMMA nanoparticles had spherical morphologies. Interestingly, a few

part of Gem-PMMA conjugates likely assembled into vesicles due to the high ratio of molecular weight of PMMA in Gem-PMMA conjugates. Significantly, another water-insoluble anti-cancer drug can be simultaneously incorporated into the core of prodrug nanoparticles via hydrophobic interaction without any unfavorable influence to the pre-conjugated gemcitabine, which can be considered as a potent strategy in combination chemotherapy. Furthermore, the obtained thiol at the extremity of prodrug amphiphile can be utilized as an active target to conjugate a target molecule such as polypeptide, or conjugate the prodrug amphiphile to other particles, for example, golden nanoparticles, quantum dots through thiol-ethylene reaction or disulfide linkage to produce a versatile nano-platform.

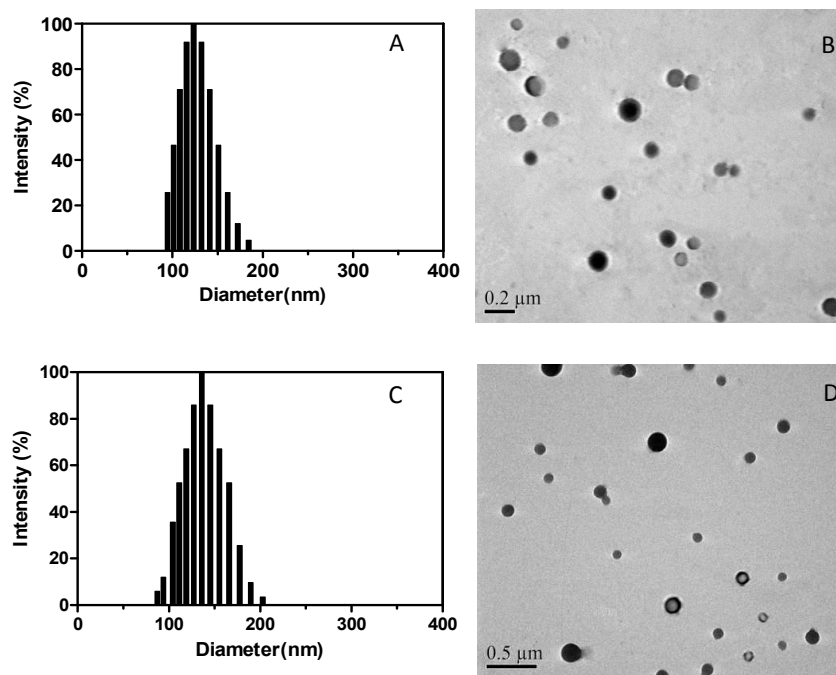


Figure 4. The diameter and TEM images of Gem-PMMA5 (A, B) and Gem-PMMA11.2 (C, D)

prodrug nanoparticles.

3.4 In vitro gemcitabine release

In vitro gemcitabine release studies were carried out under different pH environment (7.4, 6.8, and 5.5) to mimic the blood circulation environment, the extracellular matrix of tumor tissue and the lysosomal compartment within a cancer cell. The amide bond, which is often designed for enhanced oral absorption by synthesizing substrates of specific intestinal uptake transporters,⁴³ was used to link the gemcitabine molecules and PMMA segment. An amide bond is usually hydrolyzed by ubiquitous carboxyl esterases, peptidases or proteases.^{9,44} And it has been proven that substituents in the α -position of amide, such as methyl or vinyl can greatly accelerate the hydrolysis of amide at an acidic pH.⁴⁵ Thus, the hydrolysis of amide was investigated to deduce the gemcitabine release in the presence or absence of lysosomal proteolytic enzyme Cathepsin B. The hydrolysis of amide was monitored by UV-Vis spectra. As shown in Fig. 5A, the intensity of absorbance at 268 nm assigned to free gemcitabine gradually increased while that of Gem-PMMA decreased with the hydrolysis time increased, demonstrating the occurrence of amide breakage. Fig. 5B revealed that Gem-PMMA prodrug nanoparticles can sustain and control the release of gemcitabine and the hydrolysis of methyl substituted amide was pH-dependent. After hydrolysis for 72 h at pH 5.5, approximately 46.8% of initial gemcitabine was released. The presence of Cathepsin B obviously accelerated the hydrolysis of gemcitabine from Gem-PMMA conjugate and after 72 h, so the cumulative release of gemcitabine was about 71.6%. However, at pH=7.4 only 10% of total conjugated gemcitabine was liberated, indicating that Gem-PMMA conjugate

prodrug nanoparticles could effectively inhibit the burst release and subsequently decrease the deaminase by cytidine deaminase in plasma. Additionally, it seemed that the poor degradability of the hydrophobic block did not influence the gemcitabine release kinetics, which has also been observed in poly (L-glutamic acid)-paclitaxel conjugate.⁴⁶

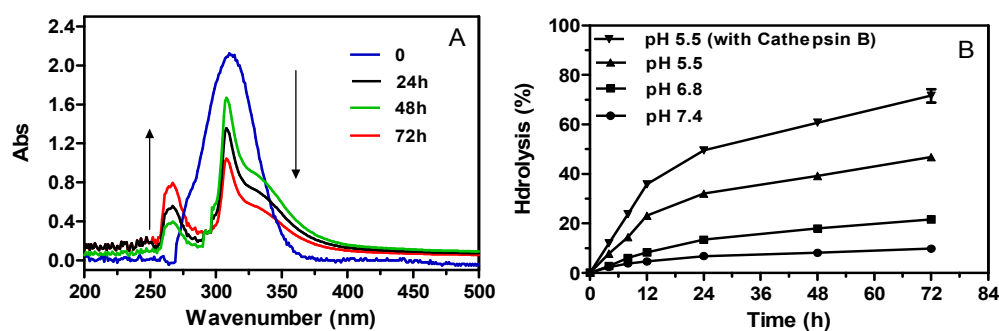


Figure 5. The UV-Vis (A) monitoring of the hydrolysis of Gem-PMMA conjugates and the cumulative release (B) of gemcitabine calculated from the hydrolysis.

3.5 In vitro cytotoxicity assay

Cytotoxic activity of gemcitabine was evaluated by incubating A549 and MCF-7 cells with free gemcitabine or gemcitabine conjugated prodrug nanoparticles for 72 h and the cell viability was determined using CCK-8 assay. It has been well recognized that poly (methyl methacrylate) based nanoparticles has no cytotoxicity to various cancer cells.⁴⁷⁻⁴⁹ Nevertheless, in this study the cytotoxicity of the PMMA derivative, prepared by RAFT polymerization via non-gemcitabine modified RAFT agent and followed by aminolysis, was implemented. The result (Fig. 6C) indicated that the PMMA derivative was not toxic to A549 and MCF-7 cells with a cell variability of above 90% compared to the control group. The formulation of Gem-PMMA

nanoparticles was found to be cytotoxic against both A549 and MCF-7 cells and the cell viability was decreased with the concentration of gemcitabine increased (Fig. 6). Both formulations can cause a median lethal when the dose was reached to approximate 2 μM . Although it was a prodrug, Gem-PMMA nanoparticles and free gemcitabine exhibited comparable cytotoxicity without any statistical significance. This was possible as it has been proven that drug-loaded nanoparticles were prone to be endocytosed through cell membrane-mediated fusion.^{14, 50, 51} In addition, deducing from the in vitro release, intracellular Gem-PMMA nanoparticles could persistently and effectively release gemcitabine molecules under the stimulation of acid environment and the catalysis of cathepsin. All these behaviors can cause the cytotoxicity of Gem-PMMA prodrug nanoparticles to A549 and MCF-7 cells.

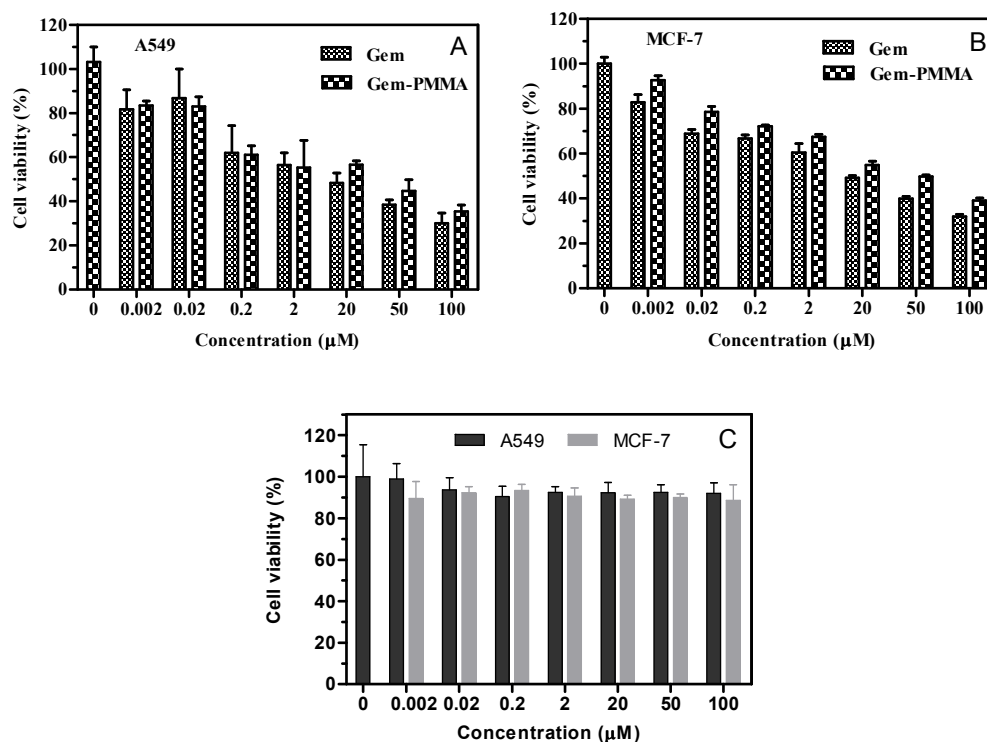


Figure 6. The in vitro cytotoxicity of gemcitabine and Gem-PMMA nanoparticles to A549 (A) and

MCF-7 (B) cells and the in vitro cytotoxicity of corresponding PMMA derivate to these cells (C).

3.6 In vivo anti-tumor activity

The in vivo anti-cancer activity of gemcitabine conjugated prodrug nanoparticles was tested in A549 cell derived xenograft model in BALB/c nude mice. The intravenous injection of gemcitabine or Gem-PMMA nanoparticles at a dose of 26 mg/kg was carried out on day 5, 8, 11 after tumor inoculation. Fig. 7A showed that untreated mice (saline 0.9%) exhibited a rapid tumor growth, with an average tumor volume of approximately 1441 mm³ at day 17. Mice treated with gemcitabine showed a similar pattern, with equivalent tumor volumes at the end of the treatment, thus demonstrating the absence of anti-cancer activity of gemcitabine in this model. In contrast, treatment of mice with Gem-PMMA prodrug nanoparticles at the equivalent dose of gemcitabine significantly reduced the tumor growth with an inhibition as high as 68%. Statistical significance (*p*-value of 0.0157) was observed with Gem-PMMA nanoaprticles treatment against the control group or Gem treatment. The change in body weight of the animals was also monitored throughout the treatment (Fig. 7B). Obviously, gemcitabine-treated mice exhibited significant weight loss (approximately 13.3%) compared to that of control group and this result highlighted the toxicity of the free-drug treatment. However, the Gem-PMMA nanoparticles-treated mice only slightly decreased the body weight of mice (approximately 3.7%). These findings indicated the efficient anti-cancer activity of gemcitabine conjugate prodrug nanoparticles and the effective alleviation of gemcitabine-related adverse effects.

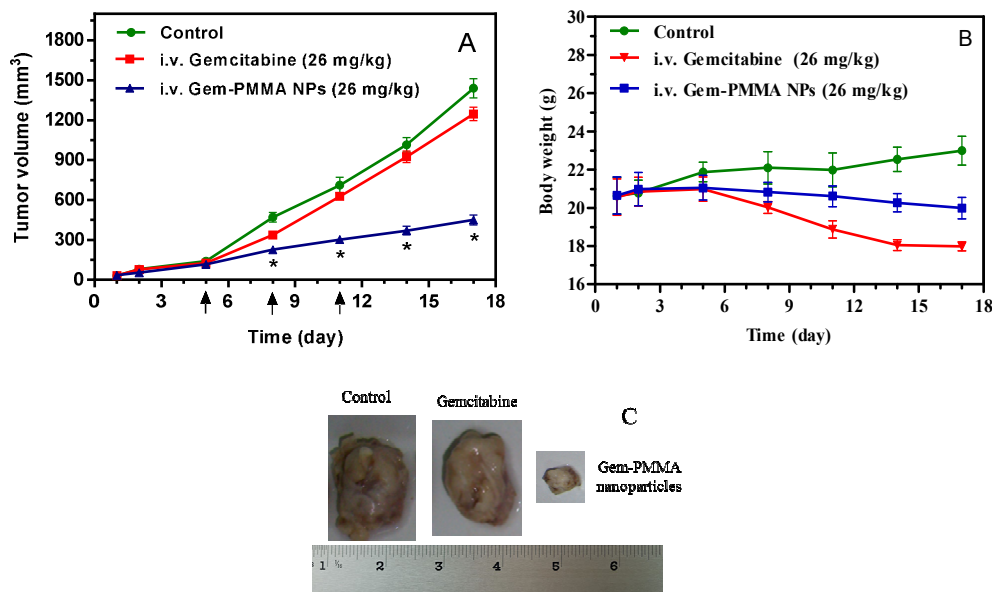


Figure 7. In vivo anti-tumor effect (A) of Gem-PMMA nanoparticles against A549-induced BALB/c nude mice, body weights of the animals (B) and representative tumor tissues for different treatment groups (C). I.v. is short for intravenous injection and the arrows indicate the injection schedule. A statistical significance was observed (* $p < 0.05$) after the first injection.

4. Discussions

Gemcitabine is a chemotherapeutic agent that was approved by FDA in 1996 as the first-line treatment for patients who have been diagnosed with locally advanced (non-resectable Stage II or Stage III) or metastatic (Stage IV) non-small cell lung cancer.^{35, 42} However, since gemcitabine is rapidly deaminated in the circulation system into its inactive metabolite 2',2'-difluorodeoxyuridin, it has a short half-life, which requires high dosage (1000 mg/m²) administration to improve its clinical therapeutic index, although adverse side effects are often a health concern. Moreover, tumor resistance against gemcitabine also occurs due to the loss of nucleoside

transporters and phosphorylation kinases that are essential for drug entry and activation within the malignant cells.

The use of prodrug has emerged as a promising drug delivery method that could potentially improve the metabolic stability of chemotherapeutic compounds, enhance their anti-tumor activities and ameliorate chemotherapy-related resistance. For targeted delivery of gemcitabine, various pharmaceutical approaches have focused on chemical modifications of the amino group at 4-(N)-position or the hydroxyl group at 5'-position of the gemcitabine molecule.³⁵ These modifications could facilitate conjugation of the drug compound with lipophilic molecules or polymeric carriers, which protect gemcitabine from plasma metabolism. Passively delivery of the drug conjugates into tumor cells is also made possible due to the lipophilic property of the conjugated polymers. Thus, several lipophilic gemcitabine conjugates including PEG-gemcitabine,²² squalenoyl-gemcitabine,⁵³ gemcitabine-polyisoprene¹² and poly(ethylene glycol)-*block*- poly(2-methyl-2-carboxyl-propylenecarbonate) - gemcitabine,⁹ have all been investigated as potential prodrugs to improve the clinical outcome of gemcitabine chemotherapy. However, several limiting factors of these delivery systems have also been reported which were caused by poor aqueous solubility, low intracellular uptake, nonspecific tumor targeting, slow drug release or low gemcitabine payload of the gemcitabine conjugates. Moreover, the lack of chemically active groups of the conjugated polymers may also limit further modifications of the gemcitabine conjugates with tumor targeting molecules, bioactive polypeptides or proteins.

Another approach was using nanoparticles to encapsulate the lipophilic gemcitabine conjugates for better anti-cancer effects. Previous studies have incorporated 4-(N)-stearoyl gemcitabine into a nanoparticle made of PEGlyated stearic acid derivative for lysosomal delivery of gemcitabine.³³ Application of this delivery system successfully prolonged the circulation time of the drug compound in comparison to native gemcitabine. Increased accumulation of gemcitabine was also observed in tumor cells, although inadequate drug payload (5%) and in vivo anti-tumor activity still need to be addressed.

In the present study, a self-assembled amphiphilic gemcitabine-PMMA conjugate was synthesized via reversible addition-fragmentation chain transfer (RAFT) polymerization, a process that enables controlled elongation of PMMA oligomers from a gemcitabine (Gem)-bearing trithiocarbonate initiator. The content of gemcitabine within the Gem-PMMA conjugates could be accurately regulated by changing the initial stoichiometry of the MMA monomers. As a result, each of the obtained amphiphiles contains a hydrophobic PMMA backbone and a hydrophilic gemcitabine tail. When dissolved in water, the Gem-PMMA conjugates undergo self-assembly to form nanoparticles with diameters ranging from 120 to 140 nm, which in comparison to PEG-Gem or other low molecular weight Gem-conjugates could increase the metabolic stability, systemic release and intracellular uptake of gemcitabine.

For anti-cancer formulations, accurate preparation of drug payload is crucial to the performance of chemotherapy. A dynamic drug payload that could be easily adjusted

according to tumors of different types, developmental stages and patient compliances would facilitate the efficacy of chemotherapy. Our results showed that the proportion of gemcitabine loading in the Gem-PMMA conjugates was more than 40% w/w, which is considerably higher than the Gem-PEGlyated amphiphilic copolymer micelles, showing a maximum payload of only 12.8% w/w.⁹ More importantly, the gemcitabine payload in our Gem-PMMA nanoparticle formulations could be accurately controlled by regulation of the molecular weight of the PMMA chain during RAFT polymerization. This on-demand regulation of gemcitabine payload is particularly significant for personalized anti-cancer treatment. Another issue is that during encapsulation, water-insoluble drugs with high drug payload tend to crystallize within the hydrophobic core of nanoparticles or other formulations, which leads to impaired drug release and consequently inhibited efficacy of chemotherapy.⁴² However, our Gem-PMMA carriers do not cause such problem since majority of the gemcitabine molecules remained in amorphous state, as illustrated by DSC and XRD.

Since gemcitabine conjugated prodrug nanoparticles are intended for intravenous administration, it is important that the Gem-containing formulations do not release active gemcitabine during plasma delivery. Premature drug release can cause plasma metabolism of gemcitabine, which in turn leads to low drug concentration and lack of efficacy of gemcitabine at the targeted tissue. Furthermore, after delivery of prodrug nanoparticles to the targeted tumors, drug internalization by lysosomes and endosomes of the tumor cells is required since lysosomes and endosomes provide an acidic and enzyme-rich environment for gemcitabine release. In order to assess the

release of free gemcitabine from our Gem-PMMA nanocarriers, drug dissociation from the polymer conjugates was measured in the presence or absence of cathepsin B (a cysteine protease) in an acidic lysosomal environment (pH 5.5), where a pH-dependent gemcitabine releasing profile was observed. However, at neutral environment, only 10% of gemcitabine was dissociated from the conjugates, which increased to 46% when the pH value decreased to 5.5. The accumulative release of gemcitabine further elevated to 70% in the presence of cathepsin B, indicating that the gemcitabine release was dependent not only on acidic hydrolysis between the gemcitabine molecules and PMMA segments, the enzymatic activity of cathepsin B is also important. Cathepsin B is a well-recognized lysosomal protease that cleaves the amide bonds between the Gem-PMMA conjugates to release gemcitabine. Previous studies have already reported a significant role of cathepsin to degrade amide bonds in order to release gemcitabine from polymeric conjugates.⁸ However, cathepsin B can only function once the Gem-conjugated amphiphilic copolymers are dissociated from its containing micelles, which is a time consuming process since the dissociation of micelles is a dynamic equilibrium with the molecularly dissolved copolymer molecules in aqueous solution. As a result, the release of gemcitabine from the hydrophobic cores of amphiphilic copolymer nanoparticles may be delayed. Indeed, a slow releasing profile was observed from a PEG-PCC-gemcitabine conjugate micelles, with an accumulative release of only 60% after 10 days,⁸ which may be accountable for its inefficient anti-tumor activity. In contrast, for our Gem-PMMA conjugates, gemcitabine acted as a hydrophilic head of Gem-PMMA. In aqueous environment,

these gemcitabine heads are completely exposed to the acidic microenvironment and the Gem-PMMA conjugates can be directly affected by cathepsin B without requirement of pre-dissociation, resulting in a much more rapid releasing process of gemcitabine. Furthermore, although degradation of the PMMA backbone is difficult, PMMA has been proven to be physiologically nontoxic and small polymer chains of PMMA can be effectively excreted.⁴⁷⁻⁴⁹ Thus, given the challenging task of in vivo delivery of water-soluble cancer drugs, our Gem-PMMA conjugates have proven to be a facile method to deliver and release active gemcitabine in a controlled and sustained manner.

To evaluate the efficacy of this Gem-PMMA prodrug nanoparticle delivery system, the anti-tumor activity of gemcitabine was examined both in vitro and in vivo. It has been well recognized tumor cell endocytosis is primarily determined by nanoparticle size and surface charge,⁵⁴ which were unaffected by the lengths of the PMMA chain within the Gem-PMMA prodrug nanoparticles. Thus, Gem-PMMA5 was used as a representative in the CCK-8 cytotoxicity assay, which demonstrated uncompromised cytotoxic activity of gemcitabine after bioconjugation with hydrophobic segment (Fig. 6). Moreover, dose-dependent cytotoxicity of gemcitabine was also observed. However, lower cell viability was observed from free gemcitabine administered A549 and MCF-7 cells in comparison to the Gem-PMMA treated groups, which was mainly due to a relatively slower cell uptake process of the Gem-PMMA nanoparticle via endocytosis. The releasing process of gemcitabine from Gem-PMMA may also be attributable to the reduced cytotoxicity of the prodrug nanoparticles since intracellular

dissociation of gemcitabine is required before its anti-cancer activity could take effects. Despite the observed in vitro cytotoxicity of the free gemcitabine, cell culture studies are inadequate to assess the potential of the Gem-PMMA in chemotherapy. Indeed, in cell culture studies, the free drug molecules directly contact to the cancer cells, whereas tumor targeting, protection of active gemcitabine from systemic enzyme degradation, mechanisms of drug uptake and its enhanced permeability and retention (EPR) effect are impossible to study in vitro due to the lack of physiological interference that commonly occurs during clinical drug administration. Hence, the anti-cancer activity of free gemcitabine and the Gem-PMMA prodrug nanoparticles was further evaluated using a xenograft mouse model with lung carcinoma. A moderate gemcitabine dosage of 26 mg/kg was selected based on previous reports.^{9, 12} Gemcitabine or prodrug nanoparticle formulations were administered via tail vein injection using BALB/c nude mice. Following administration of the same amount of gemcitabine/Gem-PMMA, better suppression of tumor growth was observed from the prodrug nanoparticles-treated groups with ameliorated gemcitabine-associated side effects. The higher efficacy of anti-tumor activity may be resulted from decreased plasma metabolism of gemcitabine within the Gem-PMMA conjugate since the prodrug nanoparticle could protect gemcitabine from cytidine deaminase-dependent deamination. Enhanced permeation and retention were also evident following Gem-PMMA application due to the nano-sized dimension of the prodrug nanoparticles. Thus, comparatively better anti-tumor activity of the Gem-PMMA prodrug nanoparticles was observed over the free drug treatment groups. Furthermore,

the anti-tumor efficacy of the Gem-PMMA was also better than that of the prodrug micelles composed of gemcitabine-PEGylated amphiphilic copolymers conjugate.⁹ Despite of the comparative antitumor efficacy compared to previous work reported by Harrison et al.,⁹ the slight decrease in body weight of experiment animals treated with prodrug nanoparticles could be attributed to the enhanced dose and more particularly to the different type of cancer and mice, which perhaps affected the pharmacokinetic property of drug. Optimizing the dosing schedule maybe an effective option to improve the pharmacokinetic–pharmacodynamic profile of gemcitabine prodrug formulation and minimize gemcitabine-associated adverse side effects. Moreover, no significant difference could be detected between the control group and free gemcitabine administered group, consistent with previous studies.^{9, 10, 22, 33} The lack of anti-tumor effect in the free gemcitabine treated animals may be due to the rapid plasma degradation of free gemcitabine, which in turn results in inadequate level of gemcitabine at the tumor site.

Taken together, gemcitabine payload of the Gem-PMMA prodrug nanoparticles could be tailor-made and enhanced via controlled living radical polymerization. The obtained gemcitabine conjugated prodrug nanoparticles were able to protect gemcitabine from rapid plasma metabolism in vivo. Controlled and sustained gemcitabine release profile was also evident, implicating a potential of the Gem-PMMA in gemcitabine delivery. In vivo analysis using BALB/c nude mice with lung cancer exhibited enhanced anti-tumor activity of gemcitabine and reduced drug-associated side effects from the Gem-PMMA treated group, indicating that the

drug conjugated PMMA prodrug nanoparticles may be a promising approach for efficient delivery of water-soluble anti-cancer drugs.

5. Conclusion

We report here a new strategy for gemcitabine-polymer prodrug conjugate preparation, which is dependent on the controlled elongation of poly (methyl methacrylate) (PMMA) by RAFT polymerization from a gemcitabine-functionalized trithiocarbonate initiator. The obtained prodrug conjugates could then self-assemble in water into narrowly dispersed nanoparticles with a diameter of 120–140 nm. The drug payload could also be tailor-made by accurately adjusting the molecular weight of PMMA oligomer, resulting in a drug payload of more than 40% w/w. In addition, instead of drug crystallization within the hydrophobic core of the nanocarriers, gemcitabine remained in the amorphous state and the release of which was pH-dependent from the conjugate nanoparticles. Gemcitabine release could also be enhanced in the presence of Cathepsin B. Results from in vitro cytotoxicity assays demonstrated efficient anti-cancer activity of the Gem-PMMA prodrug nanoparticles in human pulmonary carcinoma A549 and breast cancer MCF-7 cells. The Gem-PMMA prodrug nanoparticles also exhibited more efficient tumor suppression effects compared to free gemcitabine treated mice with ameliorated gemcitabine-associated side effects. In summary, our results implicated a potential of the gemcitabine prodrug nanoparticles in cancer chemotherapy and the drug delivery strategy outlined in this study also represents a promising approach for efficient

delivery of hydrophilic drug molecules.

Acknowledgements

This work was financially supported by Tianjin Research Program of Application Foundation and Advanced Technology (NO. 13JCYBJC39300), Chinese Postdoctoral Science Foundation (2013M540062) and National Natural Science Foundation of China (81301309). We would like to thank Professor Renjie Hu (Tianjin Institute of Medical and Pharmaceutical Science) for his collaboration of animal experiments.

References

1. X. Duan, J. Xiao, Q. Yin, Z. Zhang, H. Yu, S. Mao and Y. Li, *Acs Nano*, 2013.
2. L. Bildstein, C. Dubernet and P. Couvreur, *Adv. Drug. Deliv. Rev.*, 2011, **63**, 3-23.
3. F. Greco and M. J. Vicent, *Adv. Drug. Deliv. Rev.*, 2009, **61**, 1203-1213.
4. J. A. Barreto, W. O'Malley, M. Kubeil, B. Graham, H. Stephan and L. Spiccia, *Adv. Mater.*, 2011, **23**, H18-H40.
5. R. Haag and F. Kratz, *Angew. Chem.-Int. Edit.*, 2006, **45**, 1198-1215.
6. J.-H. Lee, K.-J. Chen, S.-H. Noh, M. A. Garcia, H. Wang, W.-Y. Lin, H. Jeong, B. J. Kong, D. B. Stout, J. Cheon and H.-R. Tseng, *Angew. Chem.-Int. Edit.*, 2013, **52**, 4384-4388.
7. J. Liu, M. Yu, C. Zhou, S. Yang, X. Ning and J. Zheng, *J. Am. Chem. Soc.*, 2013, **135**, 4978-4981.
8. V. Torchilin, *Adv. Drug. Deliv. Rev.*, 2011, **63**, 131-135.
9. D. Chitkara, A. Mittal, S. W. Behrman, N. Kumar and R. I. Mahato, *Bioconjugate chem.*, 2013, **24**, 1161-1173.
10. M. Dasari, A. P. Acharya, D. Kim, S. Lee, S. Lee, J. Rhea, R. Molinaro and N. Murthy, *Bioconjugate chem.*, 2012, **24**, 4-8.
11. D. Trung Bui, A. Maksimenko, D. Desmaële, S. Harrisson, C. Vauthier, P. Couvreur and J. Nicolas, *Biomacromolecules*, 2013, **14**, 2837-2847.
12. S. Harrisson, J. Nicolas, A. Maksimenko, D. T. Bui, J. Mouglin and P. Couvreur, *Angew. Chem.-Int. Edit.*, 2013, **52** 1678-1682.
13. D. Yang, X. Liu, X. Jiang, Y. Liu, W. Ying, H. Wang, H. Bai, W. D. Taylor, Y. Wang, J.-P. Clamme, E. Co, P. Chivukula, K. Y. Tsang, Y. Jin and L. Yu, *J. Control. Release*, 2012, **161**, 124-131.
14. B. Jung, Y.-C. Jeong, J.-H. Min, J.-E. Kim, Y.-J. Song, J.-K. Park, J.-H. Park and J.-D. Kim, *J. Mater. Chem.*, 2012, **22**, 9385.
15. P. Gou, W. Liu, W. Mao, J. Tang, Y. Shen and M. Sui, *J. Mater. Chem. B*, 2013, **1**, 284.
16. H. Song, H. Xiao, Y. Zhang, H. Cai, R. Wang, Y. Zheng, Y. Huang, Y. Li, Z. Xie, T. Liu and X. Jing,

- J. Mater. Chem. B*, 2013, **1**, 762-772.
17. S. Maiti, N. Park, J. H. Han, H. M. Jeon, J. H. Lee, S. Bhuniya, C. Kang and J. S. Kim, *J. Am. Chem. Soc.*, 2013, **135**, 4567-4572.
18. J. Rautio, H. Kumpulainen, T. Heimbach, R. Oliyai, D. Oh, T. Järvinen and J. Savolainen, *Nat. Rev. Drug. Discov.*, 2008, **7**, 255-270.
19. D. Robinson and G. Keating, *Drugs*, 2006, **66**, 941-948.
20. W. J. Gradishar, *Exp. Opin. Pharmco.*, 2006, **7**, 1041-1053.
21. R. B. Greenwald, Y. H. Choe, J. McGuire and C. D. Conover, *Adv. Drug. Deliv. Rev.*, 2003, **55**, 217-250.
22. G. Pasut, F. Canal, L. D. Via, S. Arpicco, F. A. Veronese and O. Schiavon, *J. Control. Release*, 2008, **127**, 239-248.
23. L. Seymour, *Int. J. Oncol.*, 2009, **34**, 1629-1636.
24. O. Soepenbergh, M. J. A. de Jonge, A. Sparreboom, P. de Bruin, F. A. L. M. Eskens, G. de Heus, J. Wanders, P. Cheverton, M. P. Ducharme and J. Verweij, *Clin. Cancer Res.*, 2005, **11**, 703-711.
25. H. Xiao, R. Qi, S. Liu, X. Hu, T. Duan, Y. Zheng, Y. Huang and X. Jing, *Biomaterials*, 2011, **32**, 7732-7739.
26. H. Xiao, H. Song, Q. Yang, H. Cai, R. Qi, L. Yan, S. Liu, Y. Zheng, Y. Huang, T. Liu and X. Jing, *Biomaterials*, 2012, **33**, 6507-6519.
27. H. Xiao, H. Song, Y. Zhang, R. Qi, R. Wang, Z. Xie, Y. Huang, Y. Li, Y. Wu and X. Jing, *Biomaterials*, 2012, **33**, 8657-8669.
28. D. Zhou, H. Xiao, F. Meng, S. Zhou, J. Guo, X. Li, X. Jing and Y. Huang, *Bioconjugate chem.*, 2012, **23**, 2335-2343.
29. H. Xiao, L. Yan, Y. Zhang, R. Qi, W. Li, R. Wang, S. Liu, Y. Huang, Y. Li and X. Jing, *Chem. Commun.*, 2012, **48**, 10730-10732.
30. Y. Wang, H. Wang, Y. Chen, X. Liu, Q. Jin and J. Ji, *Chem. Commun.*, 2013, **49**, 7123-7125.
31. Z. Yuan, X. Yi, J. Zhang, S. Cheng, R. Zhuo and F. Li, *Chem. Commun.*, 2013, **49**, 801-803.
32. H. Wang, F. Xu, D. Li, X. Liu, Q. Jin and J. Ji, *Poly. Chem.*, 2013, **4**, 2004-2010.
33. S. Zhu, D. S. P. Lansakara-P, X. Li and Z. Cui, *Bioconjugate chem.*, 2012, **23**, 966-980.
34. John T. Lai, D. Filla and R. Shea, *Macromolecules*, 2002, **35**, 6754-6756.
35. E. Moysan, G. Bastiat and J.-P. Benoit, *Mol. Pharm.*, 2013, **10**, 430-444.
36. M. Vandana and S. K. Sahoo, *Biomaterials*, 2010, **31**, 9340-9356.
37. S. A, S. R, B. NE, S. JM, F. MH, T. E and K. U, *Melanoma Res*, 2005, **15**, 447-451.
38. A. Laromaine, L. Koh, M. Murugesan, R. Ulijn, and M. Stevens, *J. Am. Chem. Soc.*, 2007, **129**, 4156-4157.
39. Y. Xu, Z. Liu, X. Zhang, Y. Wang, J. Tian, Y. Huang, Y. Ma, X. Zhang, and Y. Chen, *Adv. Mater.*, 2009, **21**, 1275-1279.
40. J. Yao, L. Zhang, J. Zhou, H. Liu, and Q. Zhang, *Mol. Pharmaceutics*, 2013, **10**, 1080-1091.
41. J.-K. Kim, M. D. Howard, T. D. Dziubla, J. J. Rinehart, M. Jay and X. Lu, *Acs Nano*, 2010, **5**, 209-216.
42. G. Bajaj, M. R. Kim, S. I. Mohammed and Y. Yeo, *J. Control. Release*, 2012, **158**, 386-392.
43. C. Yang, A. Dantzig and C. Pidgeon, *Pharm. Res.*, 1999, **16**, 1331-1343.
44. P. M. Potter and R. M. Wadkins, *Curr. Med. Chem.*, 2006, **13**, 1045-1054.
45. P. Xu, E. A. Van Kirk, Y. Zhan, W. J. Murdoch, M. Radosz and Y. Shen, *Angew. Chem.-Int. Edit.*, 2007, **46**, 4999-5002.

46. C. Li, *Adv. Drug. Deliv. Rev.*, 2002, **54**, 695-713.
47. V. Alt, T. Bechert, P. Steinrücke, M. Wagener, P. Seidel, E. Dingeldein, E. Domann and R. Schnettler, *Biomaterials*, 2004, **25**, 4383-4391.
48. S. M. Horowitz, C. G. Frondoza and D. W. Lennox, *J.Orthopaed. Res.*, 1988, **6**, 827-832.
49. Y.-Q. Wang, Y.-X. Sun, X.-L. Hong, X.-Z. Zhang and G.-Y. Zhang, *Mol. BioSyst.*, 2010, **6**, 256-263.
50. Y. Min, C.-Q. Mao, S. Chen, G. Ma, J. Wang and Y. Liu, *Angew. Chem.-Int. Edit.*, 2012, **51**, 6742-6747.
51. J.-Z. Du, X.-J. Du, C.-Q. Mao and J. Wang, *J. Am. Chem. Soc.*, 2011, **133**, 17560-17563.
52. T. Hoang, K. Kim, A. Jaslowski, P. Koch, P. Beatty, J. McGovern, M. Quisumbing, G. Shapiro, R. Witte and J. H. Schiller, *Lung cancer*, 2003, **42**, 97-102.
53. L. H. Reddy, J.-M. Renoir, V. Marsaud, S. Lepetre-Mouelhi, D. Desmaële and P. Couvreur, *Mol. Pharm.*, 2009, **6**, 1526-1535.
54. S. Dufort, L. Sancey and J.-L. Coll, *Adv. Drug. Deliv. Rev.*, 2012, **64**, 179-189.